Statistical model of dephasing in mesoscopic devices introduced in the scattering matrix formalism

Marco G. Pala
Dipartimento di Ingegneria dell'Informazione: Elettronica, Informatica, Telecomunicazioni, Università di Pisa
Giuseppe Iannaccone
Dipartimento di Ingegneria dell'Informazione: Elettronica, Informatica, Telecomunicazioni, Università di Pisa

M. G. Pala, G. Iannaccone, *Statistical model of dephasing in mesoscopic devices introduced in the scattering matrix formalism*, Physical Review B, **69**, pp.235304-1-235304-5 (2004).

Statistical model of dephasing in mesoscopic devices introduced in the scattering matrix formalism

Marco G. Pala[1] and Giuseppe Iannaccone[1,2]
[1]*Dipartimento di Ingegneria dell'Informazione, Università degli Studi di Pisa, via Caruso, I-56122 Pisa, Italy*
[2]*IEIIT–Consiglio Nazionale delle Ricerche, via Caruso, I-56122 Pisa, Italy*
(Received 26 November 2003; published 3 June 2004)

We propose a phenomenological model of dephasing in mesoscopic transport, based on the introduction of random-phase fluctuations in the computation of the scattering matrix of the system. A Monte Carlo averaging procedure allows us to extract electrical and microscopic device properties. We show that, in this picture, scattering matrix properties enforced by current conservation and time-reversal invariance still hold. In order to assess the validity of the proposed approach, we present simulations of conductance and magnetoconductance of Aharonov-Bohm rings that reproduce the behavior observed in experiments, in particular as far as aspects related to decoherence are concerned.

DOI: 10.1103/PhysRevB.69.235304 PACS number(s): 03.65.Yz, 11.55.−m

I. INTRODUCTION

Phase coherence of the electron wave function has a fundamental influence on the transport properties of mesoscopic devices[1] and is at the basis of several phenomena ranging from interference effects (such as Aharonov-Bohm (AB) oscillations) to weak localization (WL)[2,3] and universal conductance fluctuations (UCF).[4,5]

The fundamental quantity used to express the degree of coherence in a system is the so-called phase coherence length (or "dephasing" length) l_ϕ,[6] that is typically estimated on the basis of WL experiments in semiconductor heterostructures,[7] Si metal-oxide-semiconductor field-effect-transistors (MOSFET's),[8] metal conductors,[9] or of interference experiments in devices such as AB rings.[10,11]

Mesoscopic physics deals with devices whose sizes are smaller or comparable to l_ϕ and therefore often operate in an intermediate regime between coherent transport, in which the phase information is fully preserved, and incoherent transport. The main phase-breaking mechanisms are due to interaction of electrons with other electrons, photons, phonons, and defects such as magnetic impurities, or due to other kinds of phase-randomizing interaction with the environment. [12,13]

Therefore, it would be very useful to have a unique formalism capable to include an arbitrary degree of dephasing in the evaluation of the transport properties of a system, and to allow a seamless transition between the coherent and the fully incoherent limits.

In the case of interfering paths, an *ad hoc* random term can be added analytically to the difference between the phases accumulated in the two paths. When generic devices with two or more leads are considered, two main phenomenological models are available for including a partial degree of dephasing in the transport model: (i) insertion in the device of an additional "virtual" voltage probe[14] that can be also taken into account by properly adjusting the two-terminal conductance[15,16]; or (ii) addition of an imaginary part to the Hamiltonian in the device region.[17–19] In case (i), the seeming drawback of spatially localized decoherence can be overcome either by introducing an adequate number of virtual probes in different points of the device region,[20] or by considering the limit of a voltage lead that supports an infinite number of modes.[15] In case (ii), the carriers absorbed by the imaginary term have to be reinjected into the conductor in order to ensure current conservation.

An additional method to treat dephasing consists in including a stochastic absorption in the scattering description[21–23] through the insertion of an attenuation factor in the free propagation region. Also in this case, continuity of the probability density current requires that absorbed electrons are reinjected.

Dephasing due to the environment can be modeled by two equivalent approaches:[12] One focuses on the changes that the wave function induces on the state of the environment, and was adopted, for instance, to simulate electron conduction interacting with dynamic impurities.[24] The other addresses the phase accumulated by the interfering waves as a statistical process. In this paper, we adopt the latter perspective and propose a phenomenological model of decoherence that treats dephasing as a distributed phenomenon in the device region, ensures the conservation of current density, and allows us to evaluate the local density of states. We consider the stochastic behavior of the dephasing process and adopt a Monte Carlo averaging procedure to extract the electrical and microscopic properties of the system. We are able to vary l_ϕ and gradually move from a coherent to a totally incoherent transport regime. The model is described in Sec. II and is applied in Sec. III to evaluate the decoherence on the conductance and magnetoconductance of an AB ring.

II. DEPHASING MODEL

We include our model for dephasing in the scattering matrix formalism for the computation of the device conductance G. The conductance of a generic structure is related to the transmission probability matrix $T=t^\dagger t$ by the Landauer-Büttiker formula $G=ge^2/h\Sigma_{n,m}T_{nm}$,[25] where t is the transmission matrix, g is the spin degeneracy factor, e is the elementary charge, h is Planck's constant, and n, m run over all transverse modes contributing to transport.

The transmission matrix is obtained by computing the scattering matrix (S matrix) of the device.[26] If we subdivide the domain along the transport direction x in several slices, one for each grid point $j=1,\ldots,N_x$ in the x direction, the wave function of the electron in the jth slice ($x_j<x<x_{j+1}$) can be written as

$$\psi_j(x,y)=\sum_n \frac{\chi_{j,n}(y)}{\sqrt{|k_{j,n}|}}(a_{j,n}e^{ik_{j,n}x}+b_{j,n}e^{-ik_{j,n}x}), \tag{1}$$

where $\chi_{j,n}(y)$ is the nth transverse eigenvector of the jth slice with eigenenergies $E_{j,n}$ and the longitudinal wave vector $k_{j,n}$ is related to the total energy E by the condition $E=E_{j,n}+\hbar^2k_{j,n}^2/2m_j$. The coefficients $a_{j,n}$ and $b_{j,n}$ are obtained by imposing the continuity of the wave function and of the probability current density at the interface between the jth and the $(j+1)$th slice. The scattering matrix S_j links the incoming and the outgoing coefficients:

$$\begin{pmatrix} b_j \\ a_{j+1} \end{pmatrix}=S_j\begin{pmatrix} a_j \\ b_{j+1} \end{pmatrix}, \tag{2}$$

where $a_j(b_j)$ is the column vector of all $a_{j,n}$'s ($b_{j,n}$'s) for $n=1,\ldots,N_{\text{mode}}$, and N_{mode} is the total number of modes considered in the system. The composition between two adjacent scattering matrices[26], S_j and S_{j+1}, gives the matrix $S_j\otimes S_{j+1}$, which links a_j, b_j, a_{j+2}, and b_{j+2}. In order to compute the scattering matrix of the complete device we have to compose the matrices of all slices according to well known rules:[26] $S=S_1\otimes\cdots\otimes S_j\otimes\cdots\otimes S_{N_x-1}$.

We model the effect of decoherence as a random variation of the phase accumulated by each mode in each slice into which the device has been divided. In the absence of dephasing, mode n accumulates in slice j a phase $k_{j,n}(x_{j+1}-x_j)$; in the presence of dephasing it accumulates a phase $k_{j,n}(x_{j+1}-x_j)+\Delta\phi_{j,n}$, where $\Delta\phi_{j,n}$ is a random term obeying a Gaussian probability distribution with zero average and standard deviation σ_j; that depends on the thickness of the slice $(x_{j+1}-x_j)$ and on l_ϕ, as we shall show.

For a random choice of all $\Delta\phi_{j,n}$'s, for $j=1,\ldots,N_x-1$, $n=1,\ldots,N_{\text{mode}}$, we can compute an "occurrence" $\tilde{S}$ of the scattering matrix of the system. We take into account the probabilistic nature of dephasing, and therefore transport properties are obtained following a Monte Carlo averaging procedure over a sufficiently large ensemble of random occurrences. For typical devices, in order to obtain stable and "smooth" averages, we need to consider an ensemble of about a hundred occurrences.

For the purpose of clarity, we have described the case of two-terminal devices. However, the method can be applied without any variation for the computation of many-terminal scattering matrices.

Using some algebra it is straightforward to verify the unitarity of any $\tilde{S}$: adding the random-phase term to the scattering matrix of the jth slice corresponds to substitute the coherent matrix S_j with $\tilde{S}_j=S_j\otimes S_j^{\text{random}}$, where S_j^{random} is a scattering matrix in which the reflection matrices are zero, and the transmission matrices are diagonal, their nth element $(n=1,\ldots,N_{\text{mode}})$ being $\exp(i\Delta\phi_{j,n})$.

It is easy to verify that S_j^{random} is unitary by construction; since composition of unitary scattering matrices provides a unitary scattering matrix, each $\tilde{S}$ is unitary.

The physical reason for unitarity of $\tilde{S}$ is the conservation of the incoming current, whereas the time-reversal symmetry in the presence of a magnetic flux Φ implies the validity of the Onsager-Casimir relations[27]

$$T_{pq}(\Phi)=T_{qp}(-\Phi),\quad R_{pp}(\Phi)=R_{pp}(-\Phi), \tag{3}$$

where the labels q and p denote the leads of the system and T_{pq} is the total transmission probability from lead p to lead q (summed over all modes), and R_{pp} is the total reflection probability at lead p.[28] Once again, each S_j^{random} is symmetric and independent of the magnetic field and therefore obeys (3); it is now sufficient to observe that a composition of matrices obeying (3) still provides a matrix that obeys Onsager-Casimir relations.

Let us consider a traveling plane wave that loses phase coherence as it propagates, but conserves its modulus. One possible description of such a situation is to write the wave function as the sum of a coherent component whose amplitude decays exponentially with propagation for a length l as $e^{-l/2l_\phi}$ and of an incoherent component totally uncorrelated with the former that ensures conservation of the wave-function modulus. Another possible description is to add to the phase of the traveling wave function after a length l a random term with Gaussian distribution, zero average, and standard deviation σ.

In order to derive the relation between l_ϕ and σ, we consider the case of wave interference. First, let us consider two coherent wave functions ψ_1 and ψ_2 of amplitude unity, obtained, for example, with a beam splitter. We let them interfere again after both propagate along paths of length l. In terms of the former description the amplitude of the interfering pattern is

$$|\psi_1+\psi_2|^2_{\max}-|\psi_1+\psi_2|^2_{\min}=4\,\exp(-l/l_\phi). \tag{4}$$

On the other hand, if we write the same two wave functions with the latter description, they have amplitude unity and phases containing additional random terms ϕ_{R}^1 and ϕ_{R}^2, respectively, that are uncorrelated, and obey a Gaussian distribution with average zero and standard deviation σ. The amplitude of the interfering pattern, in this case, is

$$\langle|e^{i\phi_{\text{R}}^1}+e^{i\phi_{\text{R}}^2}|^2\rangle-\langle|e^{i\phi_{\text{R}}^1}-e^{i\phi_{\text{R}}^2}|^2\rangle=4\langle\cos(\phi_{\text{R}}^1-\phi_{\text{R}}^2)\rangle=4e^{-\sigma^2}, \tag{5}$$

where angle brackets mean statistical averaging, and the last equation has been obtained using the fact that $\phi_{\text{R}}^1-\phi_{\text{R}}^2$ is a Gaussian variable of average zero and variance $2\sigma^2$, and $\langle\cos\,\phi\rangle=\int d\phi\,\cos\,\phi\,\exp\,[-\phi^2/4\sigma^2]/\sqrt{4\pi\sigma^2}=e^{-\sigma^2}$.

By comparing (4) and (5), we obtain $\sigma^2=l/l_\phi$ that, if we consider each single slice in which the structure is partitioned, means

$$\sigma_j=\sqrt{\frac{x_{j+1}-x_j}{l_\phi}}. \tag{6}$$

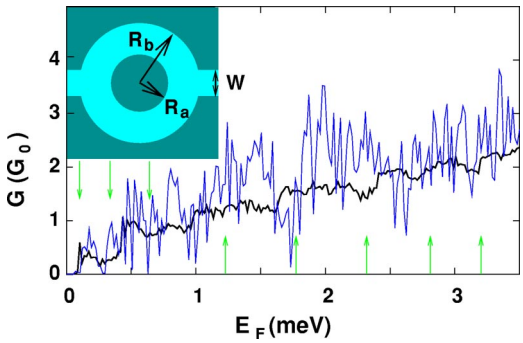

FIG. 1. (Color online) Conductance of the AB ring as a function of the Fermi level of electrons: Completely coherent regime (thin solid line), partially incoherent regime corresponding to $l_\phi = 0.3\mu$m (thick solid line). Results are averaged on 100 random occurrences. The arrows indicate the energies at which a new conducting channel in the lead is opened. Inset: the AB ring potential used in our simulations. The internal radius R_a is 350 nm, whereas the external radius R_b is 630 nm. The width of the branches W that connect the ring to drain and source is 200 nm. G_0 is the conductance quantum $2e^2/h$.

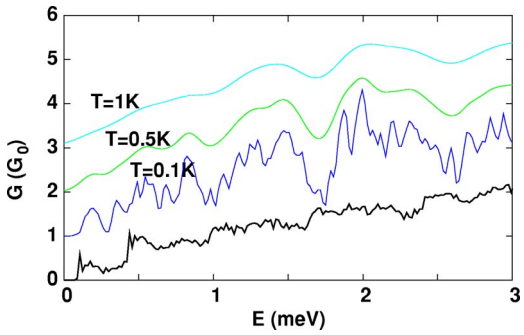

FIG. 2. (Color online) Comparison between the conductance of the AB ring at 0 K computed with $l_\phi = 0.3$ μm (thick line) and fully coherent conductances computed at finite temperature (thin lines). For clarity of presentation each line is shifted by one unit of conductance.

III. SIMULATIONS

In this section we use our proposed model for dephasing to investigate the effect of decoherence on UCF and Aharonov-Bohm oscillations in mesoscopic rings, for which experimental results are available in the literature.

The Aharonov-Bohm ring (shown the inset of Fig. 1) is broadly used to perform phase coherence measurements because it provides the possibility to obtain WL, UCF, as well as pure interference effects.[1] As far as this aspect is concerned, analytical predictions of the dephasing rate are available,[29] which agree very well with the experiments.[10]

UCF appears when an external parameter that alters the potential profile of the structure is varied. Indeed, such conductance fluctuations are obtained in experiments by varying the Fermi level E_F of the electrons through the voltage on the back gate or on a top gate. The typical amplitude of conductance fluctuations does not depend on the sample size or on the degree of disorder and is of the order of the conductance quantum $2e^2/h$ in a purely coherent transport regime.[4,5,16] If this is not the case, decoherence smears out fluctuations restoring a staircase when G is plotted versus E_F or versus the gate voltage, as shown, for example, in the experiments of Refs. 10 and 11.

We have simulated a symmetric AB ring structure defined by etching on a GaAs/AlGaAs heterostructure. With reference to the inset of Fig. 1, the internal radius of the ring is 350 nm, the external radius is 630 nm, and the width of the leads is 200 nm. Bright regions correspond to a potential energy of 0 eV, dark regions to 0.2 eV.

The thin line in Fig. 1 is the computed conductance as a function of E_F for fully coherent transport, while the thick line is the conductance corresponding to a dephasing length $l_\phi = 0.3$ μm. Results are obtained by averaging on 100 random occurrences. The fluctuations clearly present in the coherent regime are evidently smoothed out as decoherence is introduced.

In addition, as a consequence of the introduction of decoherence we are able to observe the loss of the universality in the conductance behavior, which now presents a series of noninteger plateaus. Such behavior is typically observed in experiments[10,30,31] as is due to backscattering phenomena and to scattering at the interface between one-dimensional (1D) and 2D electron gas. However, some degree of decoherence, which is always present in experiments, is required to clearly reproduce the phenomenon with simulations.

We want to emphasize that dephasing introduced by our model has a very different effect on the device conductance than energy averaging due to a finite temperature of the system. In Fig. 2 we plot the conductance of the same ring in Fig. 1 versus E_F and compare it with the thermal-averaged conductance computed in the case of fully coherent transport:

$$\bar{G}(T) = -\int dE G(E) \frac{\partial f(E,T)}{\partial E},$$

where $f(E,T)$ is the Fermi-Dirac occupation factor. As can be seen, the coherent conductance at different temperatures does not exhibit the noninteger plateaus previously observed and has a behavior qualitatively different from partially coherent conductance.

Another way to verify how dephasing influences the transport properties of the ring structure is represented by the study of magnetoconductance. In our code we have added the effects of an external magnetic field $\mathbf{B}=(0,0,B)$ perpendicular to the propagation plane xy. We adopt the transverse gauge $\mathbf{A}=(-By,0,0)$ for the vector potential $\mathbf{A}$ as described in Ref. 32. Due to the AB ring geometry the phase difference of wave functions propagating along the two branches depends on the magnetic field as $\int(\mathbf{p}-e\mathbf{A})/h\cdot d\mathbf{r}$, generating the magnetoconductance oscillations. The oscillation period can be equal to the quantum flux h/e or to the submultiples h/ne when coherent backscattering is present and the electron turns around the ring more times. As expected, decoherence suppresses the amplitude of magnetoconductance. Results for the AB ring geometry of the inset of Fig. 1 are shown in Fig. 3, where it is possible to appreciate the tran-

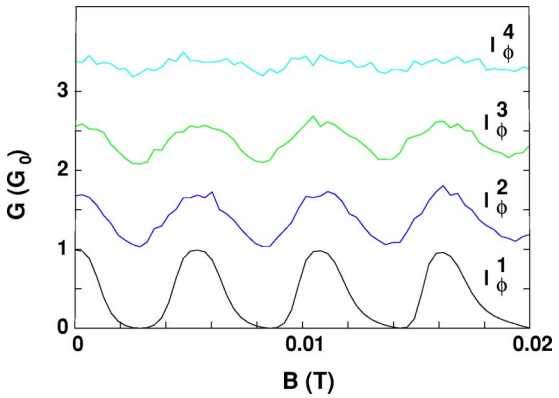

FIG. 3. (Color online) The conductance oscillations of the AB ring shown in the inset of Fig. 1 as a function of the magnetic field, for dephasing length $l_\phi^1=\infty$, $l_\phi^2=5\,\mu$m, $l_\phi^3=1\,\mu$m, $l_\phi^4=0.3\,\mu$m. G is averaged over 100 simulation runs. For clarity of presentation, each line is shifted by one conductance unit.

sition from a coherent transport regime to an only partially coherent one as l_ϕ is decreased.

In Fig. 4 we show a comparison with experimental results presented by Hansen *et al.*[10] for a symmetric AB ring with internal radius 280 nm, external radius 560 nm, and wire width 100 nm. On the left we show the fast Fourier transform (FFT) of experimental magnetoconductance oscillations (Fig. 2 of Ref. 10) for different values of temperature, while on the right we show the same quantity computed with our model for different values of the dephasing length. In both cases all frequency components are damped by decoherence. At small values of l_ϕ only the first peak corresponding to the h/e frequency is clearly visible.

It is important to verify whether the dephasing length microscopically introduced by our model through Eq. (6) agrees with the value that can be extracted from the electrical properties of the device. Following Ref. 10 we assume that the amplitude A_n of the h/ne oscillation can be written as

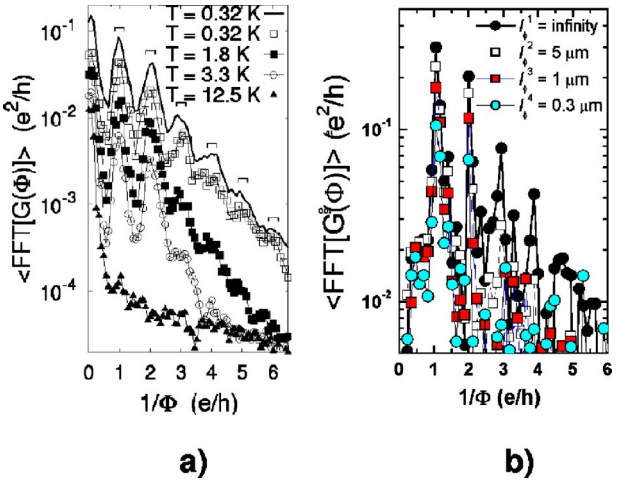

FIG. 4. (Color online) Left: fast Fourier transform (FFT) of the AB experimental oscillations measured by Hansen *et al.* (Fig. 2 of Ref. 10) at different temperatures. Right: the same FFT obtained with our simulations for values of the dephasing length $l_\phi^1=\infty$, $l_\phi^2=5\ \mu$m, $l_\phi^3=1\ \mu$m, $l_\phi^4=0.3\ \mu$m. In the simulation results, the DC component has been removed.

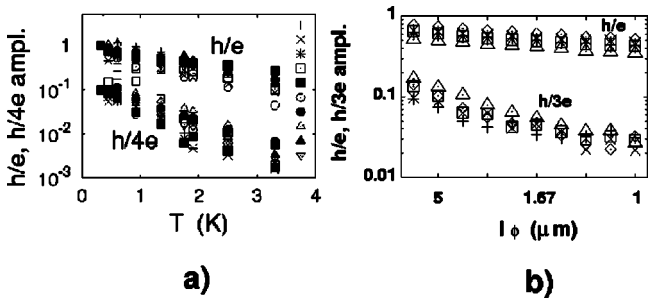

FIG. 5. Left: Measured oscillation amplitude for the h/e and $h/4e$ frequencies (Fig. 2 of Ref. 10). Right: Amplitude of the h/e and $h/3e$ oscillations plotted as a function of the dephasing length l_ϕ. Each dot corresponds to a different Fermi energy of the propagating electrons.

$$A_n \propto e^{-nL/l_\phi}, \tag{7}$$

where L is the circumference of the ring. Such assumption is confirmed by the experimental results shown in Fig. 5(a) (Fig. 2 of Ref. 10).

The FFT of the simulated oscillation amplitudes for different n exhibits an exponential dependence on l_ϕ as shown in the semilog plot of Fig. 5(b) for the cases $n=1$ and $n=3$. Both the slopes of the $h/3e$ and the h/e oscillations, according to Eq. (7), are consistent with the nominal value provided by Eq. (6). Results for $n>3$ are not reliable in the whole range of l_ϕ due to numerical fluctuations and therefore are not shown.

Finally, we emphasize the possibility of a microscopic description of the effects of decoherence in the system. In

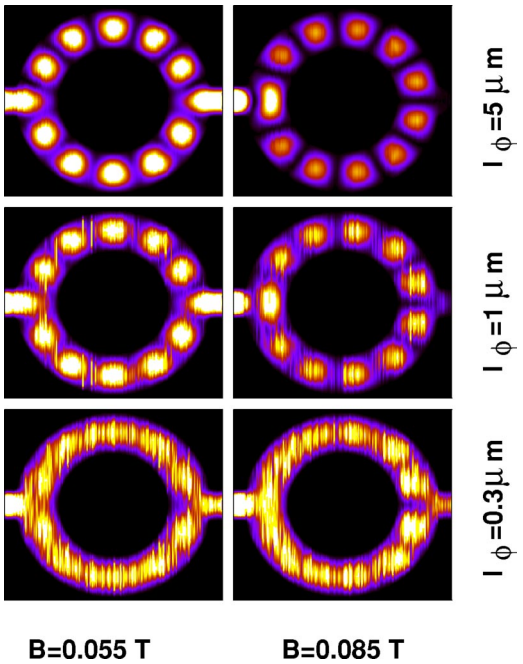

FIG. 6. (Color online) Partial density of states for different dephasing lengths in the AB ring of Fig. 1 when only the first mode is populated. The magnetic field B is 55 mT and 85 mT, corresponding to a maximum and a minimum of conductance (see Fig. 3).

Fig. 6 we show the partial local density of states corresponding to one mode injected from the left $\rho(x,y,E) \propto |\psi(x,y,E)|^2$ for three different values of l_ϕ and two different values of the magnetic field B, corresponding to the cases of maximum constructive interference ($B=55$ mT) and maximum destructive interference ($B=85$mT), as can be seen in Fig. 3. Also in this case the density of states is obtained by averaging over 100 Monte Carlo runs.

For $l_\phi=5$ μm transport is almost fully coherent, a clear pattern of nodes forms in both branches, and in the output lead we have maximum modulation of the density of states as a function of B. For smaller dephasing lengths the stationary wave pattern in the branches smooths out. In particular, for $l_\phi=0.3$ μm, when the interference pattern is almost destroyed, as can be seen in Fig. 3, the density of states is quasiconstant in the branches and in the leads.

IV. CONCLUSIONS

In this paper we have presented a phenomenological microscopic model for the simulation of dephasing in mesoscopic devices. The stochastic nature of the dephasing process is taken into account with a Monte Carlo methodology used to extract average conductance, magnetoconductance, and density of states. We have shown that the proposed method ensures the physical validity of each occurrence of the scattering matrix.

Here we want to underline the fact that the proposed method provides a unique description applicable to systems with an arbitrary degree of dephasing. This represents the main advantage of the proposed method, since common methods for determining transport properties of generic devices consider only the limit of completely coherent transport (with scattering matrix or recursive Green's functions techniques) or the limit of fully incoherent transport (with semiclassical approaches).

We have also shown that such method allows us to recover experimental results observed in Aharonov-Bohm rings, when a certain degree of decoherence is always present and responsible for some typical features, such as the noninteger conductance plateaus at zero magnetic field.

We believe that the proposed model can be very useful in understanding the effect of dephasing on the transport properties of mesoscopic devices, and enables to accurately reproduce experimental results with numerical simulations. It can also have a significant effect in assessing the effect of dephasing on the noise properties of nanoscale devices.

ACKNOWLEDGMENTS

The authors would like to thank M. Governale for interesting discussions. The work presented in this paper has been supported by the IST NANOTCAD project (EU contract IST-1999-10828), and by the SINANO Network of Excellence (EU Contract No. 506884).

[1] See, for instance, A. D. Stone, in *Physics of Nanostructures, Theory of Coherent Quantum Transport*, edited by J. H. Davies and A. R. Long (Scottish University Press and Institute of Physics, Bristol, 1992) , pp. 65–100.
[2] E. Abrahams, P. W. Anderson, D. C. Licciardello, and T. V. Ramakrishnan, Phys. Rev. Lett. **42**, 673 (1979).
[3] A. B. Altshuler, A. G. Aronov, and B. Z. Spivak, JETP Lett. **33**, 94 (1981).
[4] A. B. Altshuler, JETP Lett. **41**, 648 (1985).
[5] P. A. Lee and A. D. Stone, Phys. Rev. Lett. **55**, 1622 (1985).
[6] C. W. J. Beenakker and H. van Houten, in *Solid State Physics, Semiconductor Heterostructures and Nanostructures*, Vol. 44 (Academic Press, San Diego, 1991) pp. 1–228.
[7] B. J. F. Lin, M. A. Paalanen, A. C. Gossard, and D. C. Tsui, Phys. Rev. B **29**, 927 (1984).
[8] D. J. Bishop, R. C. Dynes, and D. C. Tsui, Phys. Rev. B **26**, 773 (1982).
[9] P. Mohanty, E. M. Q. Jariwala, and R. A. Webb, Phys. Rev. Lett. **78**, 3366 (1997).
[10] A. E. Hansen, A. Kristensen, S. Pedersen, C. B. Sørensen, and P. E. Lindelof, Phys. Rev. B **64**, 045327 (2001).
[11] S. Pedersen, A. E. Hansen, A. Kristensen, C. B. Sørensen, and P. E. Lindelof, Phys. Rev. B **61**, 5457 (2000).
[12] A. Stern, Y. Aharonov, and Y. Imry, Phys. Rev. A **41**, 3436 (1990).
[13] S. Chakravarty and A. Schmid, Phys. Rep. **140**, 193 (1986).
[14] M. Büttiker, Phys. Rev. B **33**, 3020 (1986).
[15] P. W. Brouwer and C. W.J. Beenakker, Phys. Rev. B **55**, 4695 (1997).
[16] C. W.J. Beenakker, Rev. Mod. Phys. **69**, 731 (1997).
[17] G. Czycholl and B. Kramer, Solid State Commun. **32**, 945 (1979).
[18] K. B. Efetov, Phys. Rev. Lett. **74**, 2299 (1995).
[19] E. McCann and I. V. Lerner, J. Phys.: Condens. Matter **8**, 6719 (1996).
[20] T. Ando, Physica E (Amsterdam) **20**, 24 (2003).
[21] C. Benjamin and A. M. Jayannavar, Phys. Rev. B **65**, 153309 (2002).
[22] S. K. Joshi, D. Sahoo, and A. M. Jayannavar, Phys. Rev. B **62**, 880 (2000).
[23] G. Iannaccone and B. Pellegrini, Phys. Rev. B **53**, 2020 (1996).
[24] P. A. Mello, Y. Imry, and B. Shapiro, Phys. Rev. B **61**, 16 570 (2000).
[25] R. Landauer, IBM J. Res. Dev. **1**, 233 (1957); M. Büttiker, Phys. Rev. Lett. **57**, 1761 (1986).
[26] S. Datta, *Electronic Transport in Mesoscopic Systems* (Cambridge University Press, Cambridge, 1995).
[27] L. Onsager, Phys. Rev. **38**, 2265 (1931); H. B. G. Casimir, Rev. Mod. Phys. **17**, 343 (1945).
[28] M. Büttiker, Phys. Rev. B **38**, 9375 (1988).
[29] G. Seelig and M. Büttiker, Phys. Rev. B **64**, 245313 (2001).
[30] R. de Picciotto, H. L. Stormer, A. Yacoby, L. N. Pfeiffer, K. W. Baldwin, and K. W. West, Phys. Rev. Lett. **85**, 1730 (2000).
[31] A. Yacoby, H. L. Stormer, N. S. Wingreen, L. N. Pfeiffer, K. W. Baldwin, and K. W. West, Phys. Rev. Lett. **77**, 4612 (1996).
[32] M. Governale and D. Boese, Appl. Phys. Lett. **77**, 3215 (2000).